National Journal of Antennas and Propagation, ISSN: 2582-2659 Vol. 6, No. 3, 2024 (pp. 162-173)
RESEARCH ARTICLE
HTTP://ANTENNAJOURNAL.COM

Studying the Use of Unmanned Aerial Vehicles (UAVs) for Remote Sensing and Artificial Intelligence-Based Early Warning Systems in the Event of a Flood

Zhongliang Zhang [1*], Changyuan Wang[2]
[1]*PhD candidate, Engineering Department, International College, Krirk University, Bangkok, Thailand*
[2]*Assistant Professor, Engineering Department, International College, Krirk University, Bangkok, Thailand*

KEYWORDS:
UAV remote sensing technology;
AI;
Flood disaster;
Monitoring and early warning

ARTICLE HISTORY:
Received 19.09.2024
Revised 25.10.2024
Accepted 14.11.2024

DOI:
https://doi.org/10.31838/NJAP/06.03.20

Abstract

This study investigates the monitoring and early warning technology of flood disasters, using UAV far-flung sensing science and synthetic brain algorithms. First, the science of flood disaster sensing from afar is reviewed. Next, we'll take a look at how UAV far-flung sensing scientific software for flood disaster monitoring works when combined with GIS technology. Lastly, by integrating micro-UAV and AI technologies, the study of the micro-UAV key device and the search for AI imaginative and prescient key technology are conducted, as are the key applied sciences of the micro-UAV flood catastrophe monitoring and early warning system based on AI vision. A micro-UAV's attitude is defined by its primary device search. Mindset The concept of CNN is explained and Faster RCNN is introduced in a creative and futuristic overview of important AI applications. This study paves the way for future research on early warning systems for floods that use unmanned aerial vehicle (UAV) remote sensing and artificial intelligence (AI) techniques.

Author's Email id: zhongliangzhang5490@gmail.com, chywang128@163.com

Author's Orcid id: https://orcid.org/0009-0002-2836-2583, https://orcid.org/0000-0002-8401-9256

How to cite this article: Zhang Z, Wang C. Studying the Use of Unmanned Aerial Vehicles (UAVs) for Remote Sensing and Artificial Intelligence-Based Early Warning Systems in the Event of a Flood. National Journal of Antennas and Propagation, Vol. 6, No. 3, 2024 (pp. 162-173).

Introduction

China is a predominant catastrophe country. According to the facts launched by the Ministry of Emergency Management, in the first 1/2 of 2023, China's herbal mess-ups have been, by and large, geological mess-ups such as floods, hailstorms, and different herbal disasters, which brought on a complete of 49.609 million human beings and heavy financial losses.[1] In addition to herbal disasters, accidents and public fitness and security incidents have precipitated high-quality damage, such as the outbreak of novel coronavirus pneumonia, the "March 7" cave of a lodge in Fujian Province, and the "August 12" explosion in Tianjin. These disaster events have challenged our country's emergency management and disposal levels. Today's society is increasingly showing various uncertainties and risks, and all kinds of disaster events are sudden and frequent. China's existing emergency management system has gradually exposed the early warning of some events, such as the emergency plan being needed to be more applicable and other shortcomings. However, emergency management is an important part of the national governance system and governance capacity, and it is a long-term and urgent task for China to improve the emergency management system and strengthen modern capacity building. At present, the emergency enterprise and emergency equipment, as a vital technical assurance for emergency management, are strongly supported by the state, and the "13th Five-Year Plan" for the development of the National Emergency Response System will encompass drones in the expert gear of the emergency rescue system, which potential that drones will shine in the subject of emergency rescue. UAV belongs to the aircraft

category, has the characteristics of simple operation, diverse functions, flexibility, and speed, and can meet the rescue requirements of the rescue scene. UAV is widely used and has gained rich practical experience in many fields. Applying this technical experience to emergency rescue work will help promote the construction of China's aviation emergency rescue system.

In this work, we investigate the state-of-the-art in flood catastrophe monitoring and early warning technology, building on research into UAV distant sensing science and the synthetic Genius algorithm. Our goal is to stay one step ahead of flood catastrophe warning models. First, the science of flood disasters as it pertains to distant sensing monitoring is reviewed. Next, we'll take a look at how UAV far-sensing technology works in conjunction with GIS for flood disaster monitoring. Lastly, by integrating micro-UAV and AI technologies, the study of the key applications of an AI-based micro-UAV flood catastrophe monitoring and early warning system is conducted. This includes the investigation of the micro-UAV key device as well as the investigation of the AI imaginative and prescient key technology.

Related Works

Remote sensing monitoring of flood disaster

Flood catastrophe monitoring and contrast blended with far-flung sensing and geographic data machine technological know-how (GIS) has progressively emerged as an essential lookup course for non-engineering measures of flood catastrophe administration due to its fast, well-timed, and effective spatial statistics administration and evaluation features.[2] How to make higher use of faraway sensing and geographic statistics device technology, enhance the timeliness and accuracy of flood catastrophe data, and decorate the capacity of catastrophe prevention and discount has attracted extraordinary interest from governments and specialists worldwide.[3]

Principles of faraway sensing monitoring and assessment of flood disasters

Satellite faraway sensing monitoring science developed in the Sixties has extensive coverage, quick period, and sturdy timeliness. It is now not managed via floor monitoring conditions, etc., and has been utilized more and more in flood mess-ups.[4] The key to the off-sensing monitoring science of flood catastrophe is how to extract flood catastrophe data from blended far-flung sensing electromagnetic wave information. The utility of faraway sensing technological know-how in flood monitoring wants to clear up 4 problems: multi-source faraway sensing information fusion, cloud interference elimination, correct identification of water bodies, and correct extraction of catastrophe facts[5]. Flood catastrophe evaluation aims to determine the precise regional flood catastrophe hazard and loss. Flood catastrophe evaluation consists of flood danger evaluation and loss assessment. Flood chance evaluation emphasizes the chance and viable losses of flood disasters. In contrast, flood loss evaluation focuses on quantitative estimation of social and financial effects such as casualties and property losses prompted by the aid of catastrophe. The easy technical process of the assessment is confirmed in Figure 1.

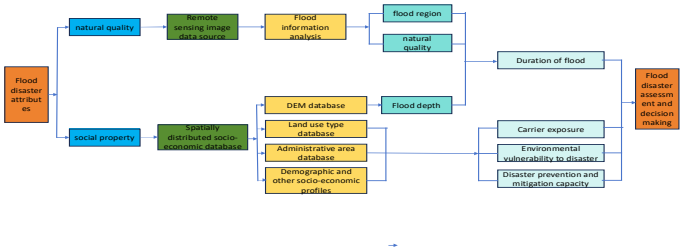

Fig. 1: Basic technical flow chart of flood disaster monitoring and assessment

Flood disaster monitoring and evaluation first need to carry out remote sensing data source selection, pre-processing, and flood inundation information extraction, and then use GIS technology superimposed spatial distribution of social and economic databases to select assessment methods and build an index system for flood disaster monitoring and evaluation. Affected by remote sensing data's temporal and spatial resolution, it is difficult for a single remote sensing data source to monitor floods effectively. Therefore, a fusion of multi-source remote sensing data to enhance image information is the key to remote sensing monitoring technology for disaster prevention and reduction.[6] Flood disaster information includes flood water bodies and social and economic loss information, among which flood water bodies information includes inundation range, duration, and inundation depth. Using remote sensing information to obtain flood water information quickly is the basic work for macro-scale flood disaster analysis and the key technology to improve the accuracy of flood monitoring.

Flood disaster assessment based on remote sensing

In flood disaster risk assessment, the frequency of historical flood inundation largely determines the magnitude of flood disaster risk. Population density and GDP data can better reflect the degree of exposure to flood disasters, and indicators such as the distribution of cultivated land and the proportion of young and old populations can better reflect flood vulnerability.[7]

Flood control standards, monitoring, early warning, and medical rescue capabilities can better reflect disaster prevention and reduction capabilities. The flood inundation range in the pixel is extracted using NOAA AVHRR, MODIS, and other remote sensing images of continuous time series, and the flood inundation frequency, since remote sensing data is available, can be obtained through superposition analysis.[8] In addition, the spatialization of flood disaster data recorded in many historical documents can expand the period of flood inundation frequency in the study area. Thus, it is helpful to determine the main distribution area of the high-value area of the risk level more accurately. On this basis, with the help of a GIS data set composed of socio-economic data and basic geographic information data, various flood disaster information of a long time series can be spatialized, disaster spatial distribution rules can be analyzed, flood disaster risk assessment and regionalization can be carried out, and evaluation results can be formed based on county (city) administrative unit and grid unit. The changing trend of flood disasters is also predicted.[9] The construction of a flood disaster database based on GIS has promoted the improvement of disaster risk assessment and management level and the in-depth research on spatial change assessment of flood risk.[10] Disaster risk assessment based on administrative regions is conducive to risk management and collection of socio-economic data.[11] Although there are community-scale risk assessments in foreign countries,[12] the basic units of such research in China are still county-level units or larger administrative units suitable for macro research, and it is difficult to propose well-targeted defense countermeasures. The grid evaluation is convenient for collecting high-precision natural environment data, but the problem of matching with administrative unit data needs to be solved urgently.

Application of UAV remote sensing in flood monitoring

An unmanned aerial vehicle (UAV) serves as the platform for remote sensing data acquisition, with a variety of imaging and non-imaging sensors serving as the primary payload.[13] The UAV remote sensing system mainly includes a UAV (flight platform system), remote sensing sensor (Earth observation sensor system), data rapid processing system, and other auxiliary systems.

UAV is an unmanned aircraft with a power device and navigation module that independently controls flight by radio remote control equipment or computer pre-programmed within a certain range.[14] UAV systems mainly include an aircraft body, flight control system, data link system, launch and recovery system, power supply system, etc. With the rapid development of UAV-related technologies at home and abroad, there are many kinds of UAV systems, wide uses, and distinctive characteristics, and there are great differences in size, quality, range, navigation time, flight height, flight speed, and tasks. According to the classification of flight platform configuration, UAVs can be divided into fixed-wing UAVs, rotor-wing UAVs, uncrewed airships, umbrella-wing UAVs, flapping-wing UAVs, etc. (Figure 3). According to the scale classification, UAVs can be divided into micro UAVs (body mass ≤7 kg), light UAVs (body mass > 7 kg and ≤116 kg), small UAVs (body mass ≤5 700 kg), and large UAVs (≥5 700 kg). Common commercial UAV platforms in China: DJI UAV is mainly based on micro and light multi-rotor UAVs. Pegasus UAV is primarily based on soft vertical take-off and landing UAVs and lightweight multi-rotor UAVs. According to the statistical analysis of Kucharczyk et al.,[15] low-cost multi-rotor UVAs with less than 30 min flight endurance are generally used in disaster monitoring (accounting for about 70%). However, within the limited flight duration, its earth observation coverage is small, and its earth observation efficiency is low when facing large-scale and multi-regional flood events.

Remote sensing sensors are an important part of the UAV remote sensing system. With the maturity of UAV platform technology, its function and performance directly determine the application effect of flood disaster monitoring. To better exploit the application potential of UAV remote sensing, relevant research institutions worldwide have carried out many research and development projects of digital lightweight and small sensors in aerial remote sensing technology. Applicable sensors such as small multispectral/hyperspectral imaging technology, synthetic aperture radar technology, UHF/VHF detection technology, and LiDAR imaging technology have been rapidly developed.

Methodology

The flood detection technology and the development of flood remote sensing technology have been studied above, and this section of the Bureau of this proposed early warning systems for floods and disasters using data collected by unmanned aerial vehicle (UAV) sensors and AI algorithms.

Research on key technologies of micro-UAV

In UAV's attitude control, there are 3 different orientation angles: heading Angle, pitch angle, and roll angle, which can indicate the UAV's attitude. Based on the above data, it is possible to express the flight posture of UAVs precisely. The micro-UAV is able to use PID arithmetic to control the dimensions of the UAV and keep its entire flying posture in order to make it safe and stable.

UAV image transmission system is composed of UAV image acquisition and sending terminal and remote host receiver. UAV image transmission system is an image transmission system based on 5.8G carrier.

The UAV global positioning system uses Beidou GPS dual-mode receiver, which can realize accurate positioning across the country.

Study on AI Vision Critical Techniques

CNN (Convolutional Neural Network) (Convolutional Neural Network) is the main model for the AI imagination and prediction machine of micro-UAV. Convolutional neural networks are a class of neural networks that are based on convolutional neural networks. The area of translation invariant classification has seen extensive application of deep convolutional neural networks in the last several years. Deep neural networks are composed of a single layer, an input layer, and an output layer.

The input level of a deep convolutional network can be either one-dimensional or multiple-dimensional. Usually, the input level of a one-dimension convolutional network is used to generate a one-dimension or two-dimension array. The dimension array is usually time or spectral sampling, and a dimensional array may additionally include more than one channel. The input layer consists of two or three dimensions of the network. The input layer of a 3-D convolution network is a 4-dimensional array. In recent years, deep convolutional neural networks have been proposed to improve their performance in order to improve their performance. In particular, the entry of an entry is expected to be normalized in a channel or time/frequency dimension before the mastery information is input into the convolution neural network. If the input is a pixel, it is possible to normalize further the unique pixel values found in the photograph to change [0-1].

Deep learning models include convolution, pooling, and deep learning. There were also complex structures in some of the more advanced algorithms, like the Inception module and the remaining block. The convolution and the pooling layer are considered models for deep learning of convolutional neural networks. Often, the order of construction of a hidden level is as follows: Input-Convolution - Pooling Level - Full Connection Level - Output Level.

Then, the convolution layer is applied for the extraction of the facts and characteristics. Each convolutional layer consists of two convolutions, each of which has a weight factor and an error range.[20]

Other RELU-like versions include slope ReLU (Leaky ReLU, LReLU), Parametric ReLU (PReLU), Randomized ReLU (Randomized ReLU, LRELU), parameter ReLU (Randomized ReLU, LRELU), Exponential Linear Unit (ELU), and so on.

To reduce the size of input data, we use the same method to deal with the facets that are produced from the convolution layer. The pooling layer utilizes accurate pooling characteristics to minimize the dimension of information. The attributes of frequent pooling are the majority of the pooling, the stochastic pooling, and the proposed pooling.[21]

The next level is the last part of a convolutional neural network, which only sends warnings to a completely unrelated layer. Data taken from previous layers will lose their 3-D form in absolute relation. Then, they are expanded into vectors and transferred to the next level by means of the activation function.[22]

In a deep convolutional neural community, the top of the output layer is usually a completely related layer, so its shape and working principle are equivalent to the output layer in an ordinary feed-forward neural network. The output level is used to identify the use of logic characteristics or normalized exponential functions. In object recognition problems, the output layer can be designed to output the central coordinates, size, and classification of the object.[23] The convolution level is composed of convolution kernel size, step size, and filling, which together determine the dimensional properties of the convolution layer. Furthermore, it is possible to obtain an accurate estimate of the cost of an input image that is significantly smaller than the input image size and the more complex it is to extract the input points.

Convolutional neural networks have a two-step training process. Archival transmission from the low to the immoderate level, also known as the beforehand transmission stage, is the first step. The unique part is the reverse propagation stage, which occurs when the penalties obtained from the present propagation are no longer consistent with the expectations. This means that the mistake is being transmitted from the extreme level to the lowest level. Figure 2 shows the results of testing the convolutional neural neighborhood's training method.

In Figure 7, the teaching gadget of the convolutional neural neighborhood is as follows:

1. The neighborhood initializes the weights.
2. The enter records are propagated beforehand via the convolution layer, undersampling layer, and fully linked layer to achieve the output value.

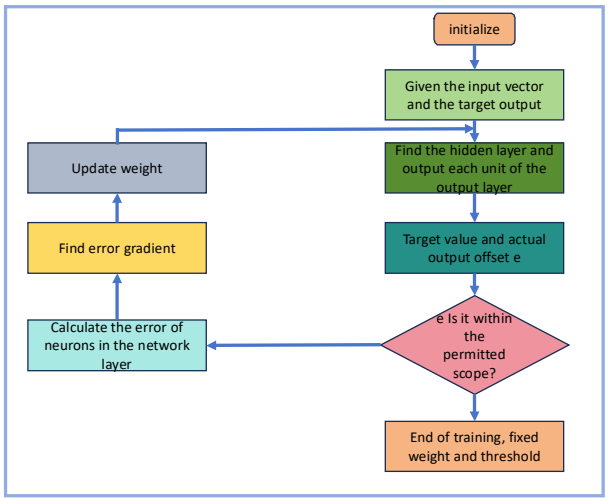

Fig. 2: Training flow of convolutional neural networks

3. Determine the discrepancy between the target value and the neighborhood's output charge.

4. In the event that the error exceeds the expected value, the network takes it upon itself to calculate the error of each layer in turn: the totally connected, under-sampled, and convolutional layers. The lesson is considered complete when the deviation from the predicted value is either the same as or significantly lower than it.

5. Update the weight in accordance with the obtained error. And then, we go on to step two.

The prepropagation technology of the convolution layer is that the input data is computed by convolution. The image has 15 inputs, and the neighboring region has a 2-by-2x1-convolution kernel; namely, the convolution kernel weights are W1, W2, W3, and W4. Then, the convolutions of the convolution kernel are shown in Figure 3. Convolutional neural networks employ a convolutional approach to convolve the entire entry photo to construct a close-by sensitive field and then carry out a convolution algorithm on it. That is, the weight matrix is weighed and combined with the picture's pixel cost (plus offset amount), and then the output is sold via an activation function.

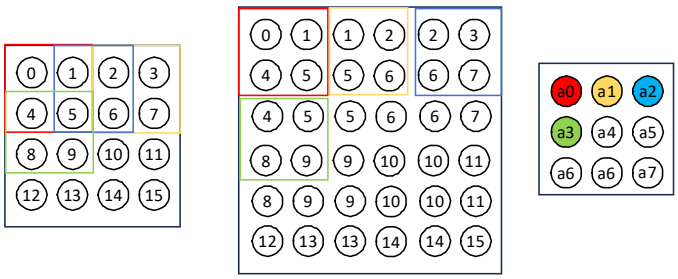

Fig. 3. Forward propagation of the convolutional layer

Then, the parameters obtained from the peak level (convolutions) are transferred to the maximum sampling level, where the data dimension can be decreased by means of the pooling operation. The usual method of grouping is shown in Figure 4. The optimal pooling approach is to select the largest amount of electric charge from the feature graph. Mean pooling is to find out the optimal price of the feature map. In this method, we first compute the probability that all the characteristic values are present in the characteristic diagram and then select one of them at random as the typical cost of the property chart, which speeds up the risk of selection.

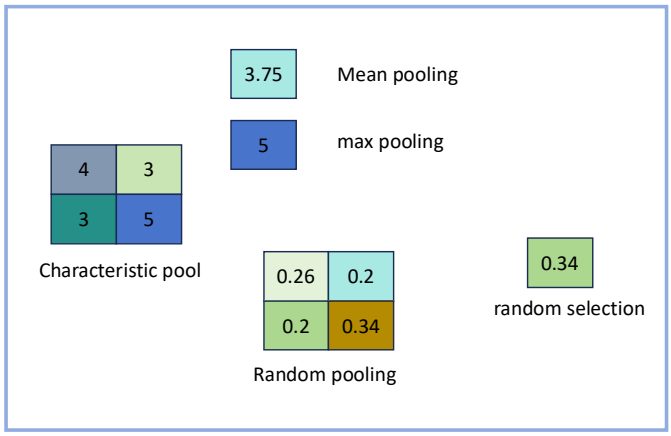

Fig. 4: Schematic diagram of pooling operation

Then, after extraction of functional maps from convolutions and sub-sampling levels, the removal of components is transferred to the fully connected layer. Then, we get the classified model by completely joining the layers and getting the closure result. In this paper, we show that the plane of the fully connected layer in the convolutional network is x1 and x2. In Figure 10, the forward propagation system is shown. The first fully connected layer has three neurons: y1, y2, and y3. Each of the three nodes has a weight matrix W. Positions b1, b2, and b3 represent the offset parts of the nodes y1, y2, and y3, respectively. It can be seen that in the absolute linked layer, the wide variety of parameters is equal to the number of nodes in the completely related layer × the variety of enter elements + the range of nodes (bias). The forward transmission system is shown in Figure 5. Once the output matrix has been acquired, it is activated by means of the exciting characteristic f (y) and passed into the following layer.

Backpropagation is used when the output of convolution networks is different from that of prediction. The difference between the result and the expectation is computed, and then the error level is returned to each level, and then the weight is replaced.

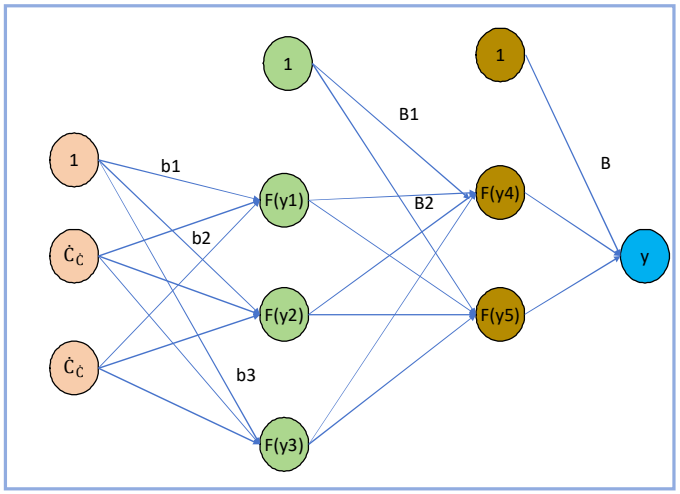

Figure 5. Forward propagation of the fully connected layer

Then, the backpropagation process is performed, and the error is transferred to the absolute relative level on the output level, which is the location of the error. The mistake of a community is caused by the neurons which constitute the net. Therefore, each neuron in a group must have a fault. It is necessary to find out which nodes in the upper level are associated with the output level and then use the weight of the nodes to get the error of each node, as shown in Figure 6.

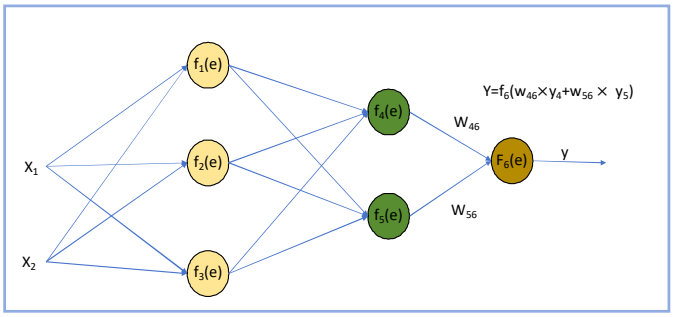

Figure 6. Error transfer process of the fully connected layer

In the reduced sampling level, the error is transferred to a higher level using the pooling method. If a maximum pooling approach is used at the sampling level, the error will be transferred immediately to the connected nodes in the upper level. If the imply pooling technique is used, the error is evenly allocated in the community of the previous layer. Furthermore, in the reduced sampling layer, since there are no parameters, it is now not necessary to substitute the weight, and it is only integrated to transfer all the errors to the higher layer effectively.

In the convolution layer, a new approach is used, which is quite different from that of a fully connected layer. In the convolution layer, the error transfer is also dependent on the convolution kernel. In this way, it is important to find the link nodes in the convolutional layer and the upper layer by means of the convolution kernel. Firstly, the error in the convolution layer is filled with all zero levels, and then it is rotated through 180 degrees. Then, by means of the twisted core, the error matrix can be filled in, and the upper level can be obtained. Figure 7 shows the convolution layer's error-switching system. The upper right of the parent represents the forward convolutions of the convolution layer, and the lower right means the transition process of the convolution layer. It can be seen from the figure that the convolution process of the error is exactly the manner of propagating forward, passing the error to the previous layer.

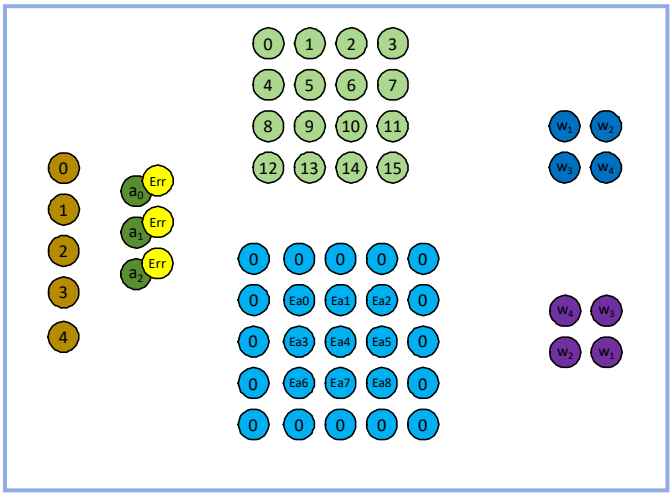

Fig. 7: Error transfer process of the convolutional layer

In this paper, we take the error matrix as a convolutive core, get the entry property, get the offset matrix of the weight, add the weight of the special convolutions core, and get the current convolution core. From Fig. 11, the weight connection of the convolution mode is precisely equal to the weight connection in the forward propagation.

The weight replace method in the totally related layer is:

1. discover the partial by-product cost of the weight; the studying charge expanded with the aid of the reciprocal of the excitation characteristic and then elevated with the aid of the entered value.
2. Add the authentic weight fee to the partial by-product price to attain a new weight matrix. The precise system is proven in Figure 9 (the activation feature in the parent is the Sigmoid function).

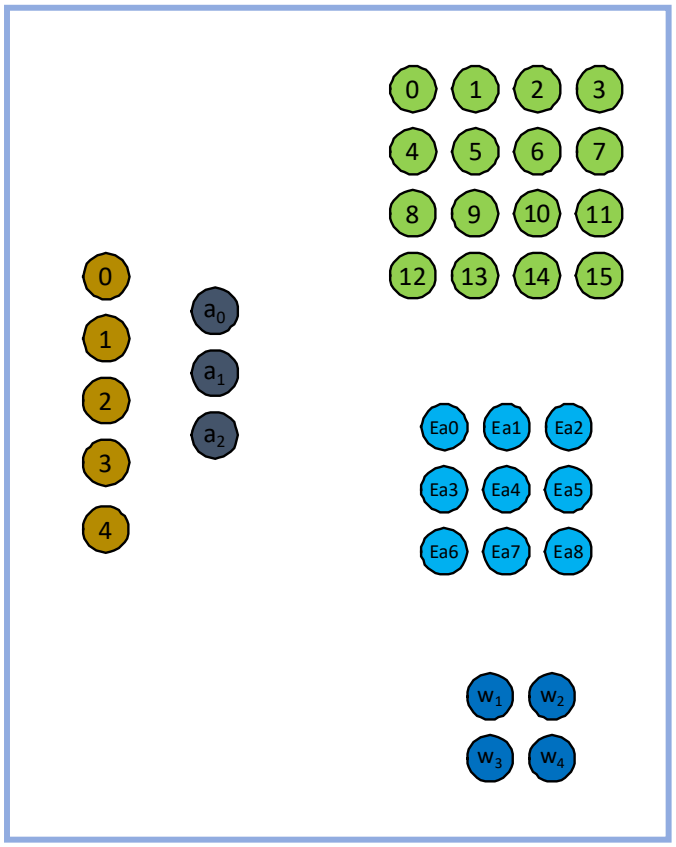

Fig. 8. The weight updating process of convolutional kernel

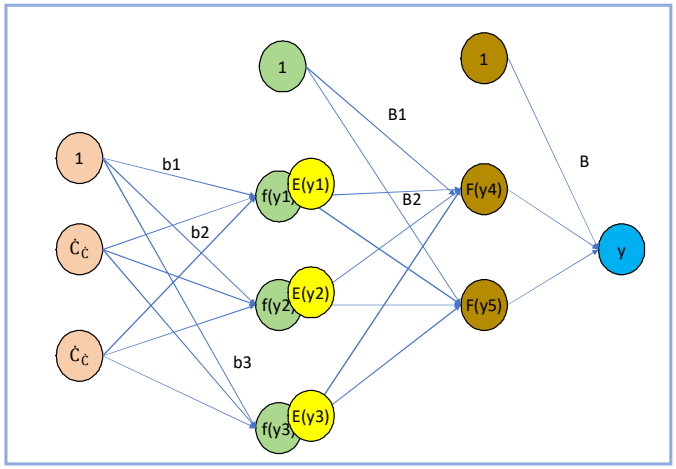

Fig. 9: Weight replaces the manner of the utterly related layer

Figure 10 shows the distinctive architecture of Faster RCNN, a CNN network target identification approach.

Faster RCNN firstly takes advantage of a series of simple conv + relu + pooling levels to get the input picture's value, which is then applied to the following RPN level and full-link layer. The RPN network is often used to

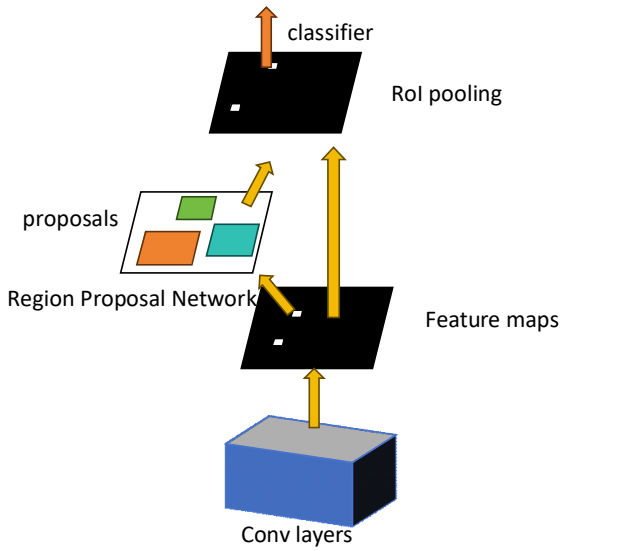

Fig. 10:. Faster RCNN's overall architecture

generate location suggestions. Firstly, we create a group of Anchor boxes, cut them, filter them, and then determine if they belong in front or back with softmax. It's either an object or not, so it's a binary class. After receiving a fixed concept feature map at the terminal level, the Roi Pooling layer uses RPN to get a rectified thought feature map. Full Link Action allows you to select and find a target. The Classifier Level will construct a Roi Pooling feature charge with a fixed dimension for complete connectivity, while Soft Max will be assigned to specific categories.

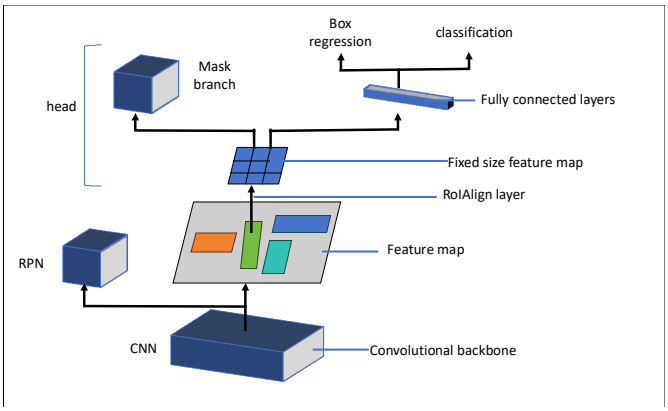

Fig. 11. Network structure of Faster RCNN

Faster RCNN, as shown in Figure 11, initially assists you in inputting images of arbitrary size, like P * Q, into this graph. Before it enters the network, the picture will undergo standardisation and scaling. Therefore, if the maximum allowed width of a picture is 600 pixels and the maximum allowed length of a photo is 1,000 pixels, then M * N = 1000 * 600. If the picture is significantly smaller, you can add zero to the region; i.e., the image

Fig. 12: (a) Regional Flood Risk Assessment (b) Floodplain Delineation

will have a black border. The Feature Map, which is 60 * 40 (1000/16 ≈ 60, 600/16 = 40), is 60 * 40 (60 × 40 = 60 × 6 × 16 = 40), This indicates that the Feature Map is 60 * 40 * 512-d in size, with 512 being the diversity and 40 being the dimensions. The Feature Map is then subjected to 3-by-3 convolutions when it comes to RPN. Likewise, a function map has a size of 60 * 40 and a value of 512. This should be done by focusing on the feature information, which is followed by two complete convolutions, namely, the size of the core is 1 * 1, the P = 0, and the step = 1.

Specify a site concept created on an RPN level (suppose there are 300 local thought fields) and a feature map created in the final level of society (60x412-d). Go through all the locations. Decrease the grid charge 16 times to map the position concept built on the basis of an original map (1000 * 600) into a function map of 60 x 40, which will then identify a location (defined as RB *) on the feature map.

The position RB * is recognized on the function map in accordance with the parameters formula _ w: 7 and formula _ h: 7. Split RB * position into 7 x 7, i.e., 49 equally sized little regions. The maximum pooling method is used for each small area to select the largest pixel as the output, thus creating a 7 * 7 feature map. Thus, according to the approach mentioned above, a number of 7-7 different maps are produced after passing through the 300 locations. Therefore, the output field is [300,512,7,7], which serves as a fully relevant entry for the next level.

Next, the feature map is fully linked, the graph of the thinking function is measured at 7 * 7, and the batch size is 300 after the ROI pooling layer. Softmax Loss and L1 Loss were added last to finish the classification and placement. Based on the whole link level and the software program output level, we can figure out which category each area belongs to, for example, person, horse, automobile, and so on, and then output the calculated probability vector. Meanwhile, the function offset box _ pred of each location concept was obtained with the help of the boundary container regression method.

Figure 12 (a) and (b) specifies the regional flood risk assessments contain the assessing the same and impact of flooding across a mentioned geographical area. This detailed examination taken several factors such as topography, water during flood, usage of land, climate pattern, and historical flood data's to assessing the vulnerability of community to flood hazard. Delineation of Floodplain, on the other side, consist of mapping the definite limit and conditions of flood where it is easily affected areas within the regions. This process uses modeling technique, consist of hydraulics and hydrological modeling's, to enhance the flood event and prediction the area closely to be affected during different flood locations.

Results and Discussion

Simulation threshold with Bayesian Network for rainfall inundation level and rainfall extent

The research presents a Simulation threshold model in which a climatic condition collaborates with a forecasting to minimum rainfall. It assumes that the extent of rainfall capacity rainfall intensity, and the duration of the rainfall may is varied, depends on the climatic condition and location may vary

Up until that point, we may consider the annual rainfall total. A model operational form is now put into place, based on the fine-adapted improvement curve model, and it is expressed as a function of compilation or enquiring tractability.

$x(n) = \int_0^t u(r)dd$ and $d(t)/d = x(i) = n(t)$. Now express C_1 as a function of $x(n)$ compiling $d_1(d) < 0;$ or inquisitive trackability, Following the idea and making the necessary adjustments makes it simple to use a specific improvement curve formula for soil permeability. A specialized improvement curve formula for C_1 is adapted and implemented. Where $x(n)$ is the numbers of samples taken in account , $'u'$ represents the supply base cost, $'r'$ represents the sampling ratio and $n(t)$ represents the number of times analysis done.

$$J = \int_o^u [E(Q - d_1 - d_2) - \beta u]dd \tag{1}$$

where, $'J'$ represents incremental in Topographical elevation, $'E'$ represents Soil permeability, $'Q'$ represents price of the Rainfall duration, d_1 represents the land cover type,.

$$\dot{y} = u \tag{2}$$

where, $\dot{y}$ represents the rate involved with a Vegetation density.

$$0 \le u \le a, m(0) = m_0 = 1 \tag{3}$$

As previously stated, ' a ' represents the Drainage network density, where $'m'$ is a value between $'0'$ and $'u'$, m_0 represents the value between $'0'$ and $'u'$ when Slope gradient exceeds. To solve the first question $(Q1)$, in optimal control theory, the maximum principle is used, and the Hamiltonian provides justification for this.

$$G = B(p - d_1 - f^m) - \beta u + \alpha u \tag{4}$$

where, $'G'$ represents the linear function of $'u'$, $'B'$ represents the optimization evaluation criterion, $'p'$ represents the process parameters, f^m denotes the Antecedent soil moisture and α represents the Stream flow velocity and the breakdown analysis. Since the defined optimisation criteria are inapplicable to a similar function of, a differentiation of Eqn. (4) is necessary to provide an optimal solution., i.e. $\delta n / \delta u = 0;$ or it is needed to validate the essential predicament for perfect solutions, First find $\delta n / \delta u = -\beta + \alpha$ and determine the binary solution is represented as:

$$u^* \begin{cases} \beta & f \quad \alpha > \beta \\ 0 & f \quad \alpha < \beta \end{cases} \tag{5}$$

where, u^* denotes the maximum utilization of the Channel cross-sectional area. Utilizing the essential requirement of the maximum principle for analyzing the change in Urbanization level

$$\alpha = \partial n / \partial x = B * l * I * z^{j-1} \tag{6}$$

where, ∂n and ∂x represents the change in Rainfall variability and Soil compaction $'l'$ represents the Predictive analysis and $'z'$ represents the Basin geomorphology and $'I'$ represents the transition from conventional. Since $\alpha < 0$ always keeps, aware extra characteristics of α (i) it represents the supplementary value of $x(n)$ (ii) $\beta(k) = 0$ because $x(n)$ is gone null and it is a continuous method i.e., $\alpha(t) \ge 0$ and $\alpha < 0$. Eqn. (5) states that there exists a time point S^* such that $\alpha(S^*) = \beta$, $0 \le S^* \le K$, and then

$$u^*(t) = \begin{cases} 0, & 0 \le s \le s^* \\ 0, & s^* < s \le S \end{cases} \tag{7}$$

where, s^* represents the Groundwater level, $u^*(t)$ represents maximum utilization of Reservoir capacity $'t'$, s^* and $'s'$ represents the Land surface temperature and forecasting (product), $'K'$ represents maximum production ratio. According to Eqn. (2), the point of equilibrium transforms at the point where it transforms to the mid-region.

$$x^*(n) = \begin{cases} b + 1, & 0 \le q \le q^* \\ b^* + 1, & q^* < q \le Q \end{cases} \tag{8}$$

where, $x^*(n)$ represents the demand structure in Bayesian mean value, b and b^* represents the Bayesian time mean and iterative Bayesian mean, $'q'$ and q^* represents the Bayesian ratio and their Iterative mean. Evaluate q^* by taking into the point for bi-polar points at the same intersection of points $\alpha(t^*) = \beta$ and $\alpha(Q) = 0$ from Eqns. (6) and (7) for $q^* \le q \le Q$.

Simulation calculation of evacuation channels and shelters in the event of floods.

Using computational simulations, we analyze optimal evacuation routes and shelter placements to enhance flood response preparedness. By modeling various

scenarios, we ensure efficient resource allocation and community safety during flood emergencies.

$$C = \{f_1, f_2, f_3 \ldots\ldots f_m\}_{1m} \quad (9)$$

$$F = \{C_1, C_2, C_3 \ldots\ldots C_m\}_{1n} \quad (10)$$

All of the criteria need to be on the same scale of measurement before they can be combined. The least desirable result is denoted by "0" and the most desired outcome is given by "1" among n categorical criteria. For results that ought to be limited, a score of "-1" is assigned.

$$\forall f_m,\ i = \{1,2,3,\ldots..n\}\ and\ m = \{1,2.3\ldots..m\} \quad (11)$$

Where $\forall f_m$ uses the supplied data, a model for the flood risk, and a model for traffic microsimulation to determine the true worth of a criteria. In certain cases, a lower value indicates a better fit; for example, in the case of structures, a lower age indicates a better fit. To keep "0" representing the worst case scenario and "1" the best case scenario for these criteria, we may use the following formula:

$$y_f^{\dot{c}} = 1 - x_{\dot{c}}^{fn} \quad (12)$$

By using this method, we can get more specific results than if we just gave each criteria a fixed number of categories. To get an appropriateness score, we add together the scores from all the criteria $y_f^{\dot{c}}$ for a facility $x_{\dot{c}}^{fn}$ according to equation.

Practical verification

In order to test the prediction effect of the model proposed in this paper, a flood in Yangshuo County is selected for validation.

Data sources

Rainfall, water level and flow data from rainfall, water level and hydrological stations in the study area, as well as spatial data such as DEM, soil type, land use, measured topography of key areas, hydraulic structures, flood scar data, etc. were collected. The Longtoushan water level station was built in 2021 and is located about 3 km upstream of the Yangshuo hydrological station. In this paper, based on the 10 floods monitored by the Longtoushan water level station and Yangshuo hydrological station, the water level correlation relationship between the Longtoushan water level station and Yangshuo hydrological station is constructed by using the corresponding level method, and the surface line of the water level of the Longtoushan station and the flood data before the station was built are supplemented with water level data of the Yangshuo hydrological station

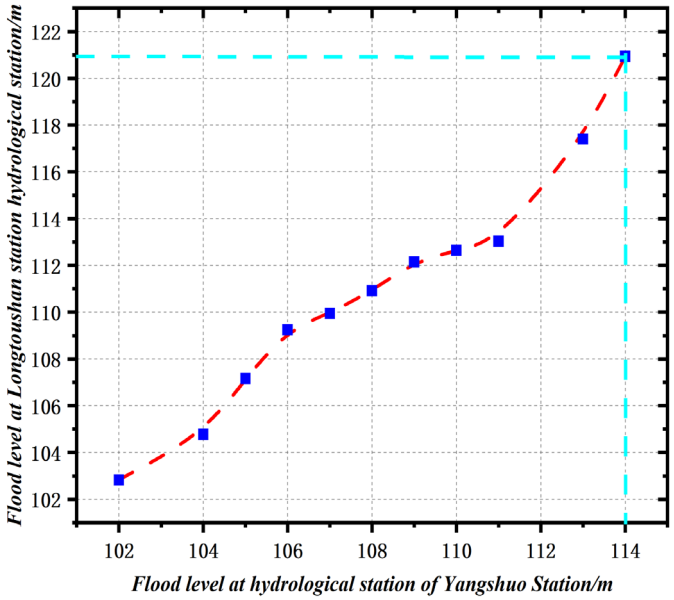

Fig. 13: Hydrological information

(see Figure 13). (see Figure 13).As shown in Fig. 14, the average 24-h rainfall in the 13 rainfall stations in the upper basin was 214.8 mm, and the average maximum 3-h continuous rainfall was 120.7 mm, which was equivalent to a one-in-20-year rainstorm. At the same time as the torrential flooding in Tianjia River, the Li River also suffered a flood peak of more than one in 20 years, and the flood peak level at Yangshuo Hydrological Station reached 113.58m, exceeding the warning level by 4.08m.

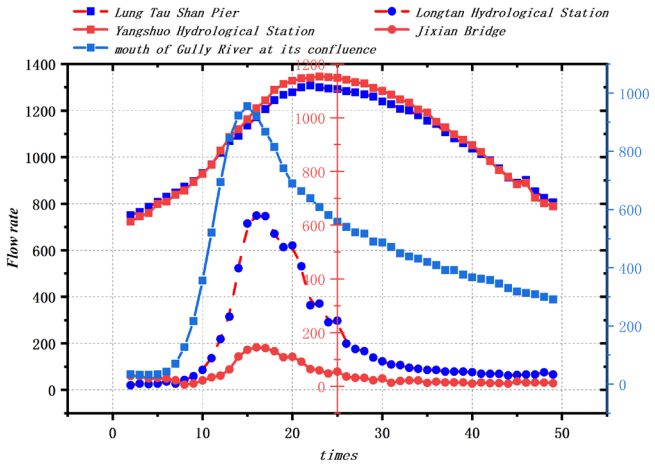

Fig. 14: Water level in Yangshuo County

Figure 15 shows the measured and predicted flood levels at various important locations in Yangshuo County, from which it can be seen that the measured and predicted flood levels are basically close to each other, which indicates that the prediction model proposed in this paper is able to accurately detect and predict flood disasters.

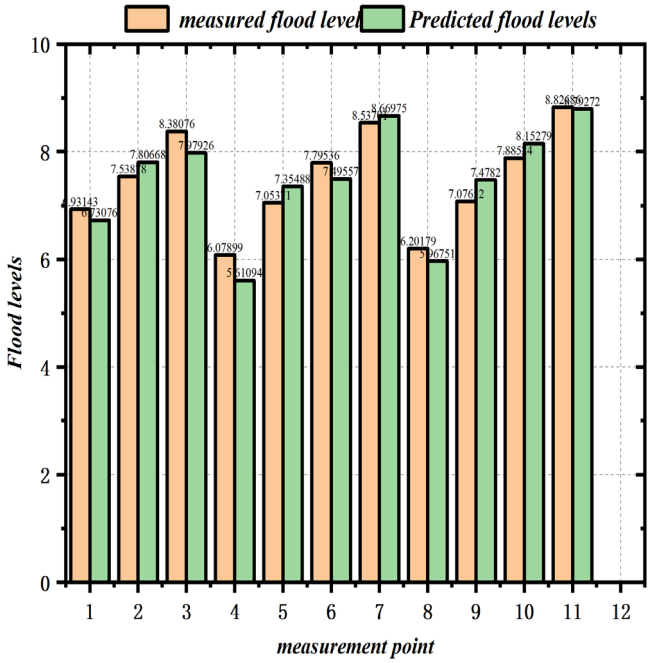

Fig. 15: Comparison of measured and predicted results

Conclusion

This thesis focuses on the research of UAV's remote sensing technique and AI arithmetic in this thesis.

First, the technical knowledge of remote sensing for flood disasters is summed up. Based on checking the principle of remote sensing monitoring and evaluating, this paper analyses and sums up the existing studies from remote sensing data and technology of remote sensing for flood disasters and puts forward the main problems in remote sensing monitoring and comparing.

Secondly, the application of remote sensing UAV in flood disaster monitoring was analyzed by combining Geographical Facts Apparatus (GIS). Because of their low efficiency and poor adaptive capability, UAVs can not satisfy the demand for large-scale emergency monitoring of flood disasters, so the remote aerial vehicle community, which is far off sensing and technological know-how, has become the cutting-edge improvement trend.

At last, micro-UAV and artificial intelligence techniques are used to research the micro-UAV disaster detection and early-warning system, which is mainly built on artificial intelligence and foresight, which includes searching for a micro-UAV keychain and searching for artificial intelligence and foresight critical techniques. In general, the key to finding a micro-UAV is to define the attitude angle. Search for Main Applications of Artificial Intelligence Imagination and Foresight mainly explains CNN's principle and presents Faster RCNN. This provides a basis for a future search in the field of disaster surveillance and early warning, which is entirely based on remote UAV remote sensing and artificial intelligence.

References

[1] Yin, N., Liu, R., Zeng, B., & Liu, N. (2019, April). A review: UAV-based Remote Sensing. In *IOP Conference Series: Materials Science and Engineering* (Vol. 490, p. 062014). IOP Publishing..

[2] Aasen, H., Honkavaara, E., Lucieer, A., & Zarco-Tejada, P. J. (2018). Quantitative remote sensing at ultra-high resolution with UAV spectroscopy: a review of sensor technology, measurement procedures, and data correction workflows. *Remote Sensing*, *10*(7), 1091.

[3] Glago, F. J. (2021). Flood disaster hazards; causes, impacts and management: a state-of-the-art review. *Natural hazards-impacts, adjustments and resilience*, 29-37.

[4] Pajares, G. (2015). Overview and current status of remote sensing applications based on unmanned aerial vehicles (UAVs). *Photogrammetric Engineering & Remote Sensing*, *81*(4), 281-330.

[5] Mohd Noor, N., Abdullah, A., & Hashim, M. (2018, July). Remote sensing UAV/drones and its applications for urban areas: A review. In *IOP conference series: Earth and environmental science* (Vol. 169, p. 012003). IOP Publishing..

[6] Preethi Latha, T., Naga Sundari, K., Cherukuri, S., & Prasad, M. V. V. S. V. (2019). Remote sensing UAV/drone technology as a tool for urban development measures in APCRDA. *The International Archives of the Photogrammetry, Remote Sensing and Spatial Information Sciences*, *42*, 525-529.

[7] Sharma, T. P. P., Zhang, J., Koju, U. A., Zhang, S., Bai, Y., & Suwal, M. K. (2019). Review of flood disaster studies in Nepal: A remote sensing perspective. International journal of disaster risk reduction, 34, 18-27.

[8] Everaerts, J. (2008). The use of unmanned aerial vehicles (UAVs) for remote sensing and mapping. The International Archives of the Photogrammetry, Remote Sensing and Spatial Information Sciences, 37(2008), 1187-1192.

[9] WANG, K., YANG, P., LÜ, W. S., ZHU, L. Y., & YU, G. M. (2020). Current status and development trend of UAV remote sensing applications in the mining industry. Chinese Journal of Engineering, 42(9), 1085-1095.

[10] Bhardwaj, A., Sam, L., Martín-Torres, F. J., & Kumar, R. (2016). UAVs as remote sensing platform in glaciology: Present applications and prospects. Remote sensing of environment, 175, 196-204.

[11] Mohsan, S. A. H., Khan, M. A., & Ghadi, Y. Y. (2023). Editorial on the Advances, Innovations, and Applications of UAV Technology for Remote Sensing. Remote Sensing, 15(21), 5087.

[12] Salamí, E., Barrado, C., & Pastor, E. (2014). UAV flight experiments applied to the remote sensing of vegetated areas. Remote Sensing, 6(11), 11051-11081.

[13] Gang, S. U. N., Wenjiang, H. U. A. N. G., Pengfei, C. H. E. N., Shuai, G. A. O., & Xiu, W. A. N. G. (2018). Advances in UAV-based multispectral remote sensing applications. Nongye Jixie Xuebao/Transactions of the Chinese Society of Agricultural Machinery, 49(3).

[14] Rokhmana, C. A. (2015). The potential of UAV-based remote sensing for supporting precision agriculture in Indonesia. Procedia Environmental Sciences, 24, 245-253.

[15] Shi, Y., Bai, M., Li, Y., & Li, Y. (2018, February). Study on UAV remote sensing technology in irrigation district informationization construction and application. In 2018 10th International Conference on Measuring Technology and Mechatronics Automation (ICMTMA) (pp. 252-255). IEEE.

[16] Tingsanchali, T. (2012). Urban flood disaster management. Procedia Engineering, 32, 25-37.

[17] Jonkman, S. N., & Kelman, I. (2005). An analysis of the causes and circumstances of flood disaster deaths. Disasters, 29(1), 75-97.

[18] Islam, R., Kamaruddin, R., Ahmad, S. A., Jan, S., & Anuar, A. R. (2016). A review of the mechanism of flood disaster management in Asia. International Review of Management and Marketing, 6(1), 29-52.

[19] Munawar, H. S. (2020). Flood disaster management: Risks, technologies, and future directions. Machine Vision Inspection Systems: Image Processing, Concepts, Methodologies and Applications, 1, 115-146.

[20] Price, R. K., & Vojinovic, Z. (2008). Urban flood disaster management. Urban Water Journal, 5(3), 259-276.

[21]Zhang, J., Zhou, C., Xu, K., & Watanabe, M. (2002). Flood disaster monitoring and evaluation in China. Global Environmental Change Part B: Environmental Hazards, 4(2), 33-43.

[22] Zhou, Z., Liu, S., Zhong, G., & Cai, Y. (2017). Flood disaster and flood control measurements in Shanghai. Natural Hazards Review, 18(1), B5016001.

[23] Yin, H., & Li, C. (2001). Human impact on floods and flood disasters on the Yangtze River. Geomorphology, 41(2-3), 105-109.

[24] Zain, Z. (2025). Exploring the field of mechatronics: Scope and future. Innovative Reviews in Engineering and Science, 2(1), 45-51. https://doi.org/10.31838/INES/02.01.05

[25] Borhan, M. N. (2025). Exploring smart technologies towards applications across industries. Innovative Reviews in Engineering and Science, 2(2), 9-16. https://doi.org/10.31838/INES/02.02.02

[26] Prasath, C. A. (2024). Cutting-edge developments in artificial intelligence for autonomous systems. Innovative Reviews in Engineering and Science, 1(1), 11-15. https://doi.org/10.31838/INES/01.01.03

[27] Kavitha, M. (2024). Energy-efficient algorithms for machine learning on embedded systems. Journal of Integrated VLSI, Embedded and Computing Technologies, 1(1), 16-20. https://doi.org/10.31838/JIVCT/01.01.04

[28] Priya, S., & Vijayan, M. (2017). Automatic street light control system using WSN based on vehicle movement and atmospheric condition. International Journal of Communication and Computer Technologies, 5(1), 6-11.

[29] Manon Mary, A., Bhuvaneswar, M., Haritha, N., Krishnaveni, V., & Punithavathisivathanu, B. (2019). Design of automatic number plate recognition system for moving vehicle. International Journal of Communication and Computer Technologies, 7(1), 1-5.

[30] Al-Yateem, N., Ismail, L., & Ahmad, M. (2024). A comprehensive analysis on semiconductor devices and circuits. Progress in Electronics and Communication Engineering, 2(1), 1–15. https://doi.org/10.31838/PECE/02.01.01